mathematics

MDPI

Article

Turing Instability and Spatial Pattern Formation in a Model of Urban Crime

Isabella Torcicollo [1,†] and Maria Vitiello [2,*,†]

[1] Istituto per le Applicazioni del Calcolo "M. Picone", CNR, Via Pietro Castellino 111, 80131 Naples, Italy; isabella.torcicollo@cnr.it
[2] Dipartimento di Meccanica, Matematica e Management (DMMM), Politecnico di Bari, Via Orabona 4, 70126 Bari, Italy
* Correspondence: maria.vitiello@poliba.it
† These authors contributed equally to this work.

Abstract: A nonlinear crime model is generalized by introducing self- and cross-diffusion terms. The effect of diffusion on the stability of non-negative constant steady states is applied. In particular, the cross-diffusion-driven instability, called Turing instability, is analyzed by linear stability analysis, and several Turing patterns driven by the cross-diffusion are studied through numerical investigations. When the Turing–Hopf conditions are satisfied, the type of instability highlighted in the ODE model persists in the PDE system, still showing an oscillatory behavior.

Keywords: crime model; self- and cross-diffusion; stability analysis; Turing patterns; Turing–Hopf bifurcation

MSC: 35Q92; 03C45; 35B32

1. Introduction

Crime and criminal activities have a wide influence on society and its development. Criminal activities not only endanger the safety of the population, but also slow down the economic process of the community. Various factors contribute to committing crime, for example, immigration of criminals and the learning of criminal behavior through interactions between criminally predisposed individuals and delinquent individuals. It is often observed that contact with criminal and delinquent individuals can produce criminal behaviors in the individuals involved and stimulate them to commit a crime [1]. Numerous scholars have conducted empirical and practical studies on various aspects of crime growth and prevention. Just as some examples, in [2], the author examined and discussed the trend and models of robbery and its various consequences in Ghana between 1982 and 1983; in [3], the authors studied the socioeconomic and demographic factors that influenced the spread of crime in Germany and found that higher economic well-being corresponds to higher crime rates.

Economic investigations into the importance of the spread of crime in society took off in the late 1960s when several economists (a small sampling includes [3–6]) turned their attention to the field of crime. In [4], a model, based on the theory of deterrence, predicted how changes in the probability and severity of sanctions may affect crime. In [3], considering a time allocation model, a descriptive analysis of crime and the potential factors contributing to crime in Germany are given. In [5], the relationship between crime and geographic space is explored, in relation to property crimes and violence, using population density in United States. The containment of the spread of crime in urban societies remains a major challenge. Empirical evidence suggests that crimes may be recurrent and proliferate if left unchecked; therefore, any kind of investigation can provide information or tools that may prove useful in its prevention and control. Mathematical

check for updates

Citation: Torcicollo, I.; Vitiello, M. Turing Instability and Spatial Pattern Formation in a Model of Urban Crime. *Mathematics* **2024**, *12*, 1097. https://doi.org/10.3390/math12071097

Academic Editor: Nikolaos L. Tsitsas

Received: 6 March 2024
Revised: 28 March 2024
Accepted: 4 April 2024
Published: 5 April 2024

modeling is a powerful tool that has been employed and developed to examine the spread of crime. One of the main targets to be achieved is to understand the conditions that allow crime to disappear from or persist within a community. Recent research has highlighted that applied mathematics may help us to understand criminal activity. Differential equations, the self-exciting point process, agent-based modeling and adversarial evolutionary games are different approaches to modeling crime activity. The study of the dynamics of the spread of crime is not untouched by predator–prey dynamics. It is a well-known fact that the interaction of criminally minded individuals with non-criminal individuals can be represented as the interaction of a predatory population with a population of prey. There are various useful studies that have dealt with quantitative models of crime which are able to represent the behavior of interacting populations in relative societies [7–10]. In particular, in [7], the authors analyzed a system of three ordinary differential equations to account for the time evolution of three sociological species, called owners, criminals and security guards. In [8], a model is constructed, based on the well-known predator–prey model, to analyze the interaction between the criminal population and the non-criminal one. Furthermore, a law enforcement term, an important part of any country's political and social systems, is incorporated in the model, and its effect is studied. The elimination or the persistence of crime is discussed via two parameters, law enforcement and the saturation constant. In [10], a diffusion-type differential equations model that captures the dynamics that describe the behavior in time of serious and minor crime is studied, and numerical solutions are compared with the crime data for the Greater Manchester area, highlighting a satisfactory agreement. In [11], a deterministic mathematical model based on nonlinear ordinary differential equations, considering education programs as a valid means of estimating the population-level impact on crime prevalence, is studied. The model is fitted with prison data (reported from July 2021 to June 2022) by the State of Illinois in the United States.

In recent years, there has been increasing interest in developing mathematical tools to understand and predict the spatial patterns of urban crime [12–19]. Several researchers have determined suitable models for analyzing intervention strategies that decrease delinquent behavior and promote social development. As a first modeling step, the population is spatially distributed over a geographical region in a homogeneous manner; only temporal variability is considered under the scheme. The formation of crime clusters suggests that criminally minded individuals do not always distribute themselves uniformly in space and time but often congregate in small clusters. Many criminal events, such as those relating to drugs, robberies, burglaries, etc., often originate from situations of aggregation or particular distributions. In fact, the composition or the distribution of the population has a relevant impact on the propagation of crime within the society. Although criminality is an aspect now present in all societies, some places have a greater propensity for crime than others. For example, data on residential burglaries show high-crime places bounded by low-crime areas. Several studies indicate that crime in a place involves more crime in that and neighboring places, leading to residential burglary hotspots; this finding emerged from real data. The observation that residential burglaries are not spatially homogeneously distributed and that certain neighborhoods have a greater propensity for crime than others led Short et al. [15,16,20] to study the dynamics of residential burglary hotspots. In particular, starting from the discrete system, the authors derived a continuum model; the two approaches are in good quantitative agreement for large system sizes. Through a linear stability analysis, they found the parameter values leading to the formation of stable hotspots.

Among the various approaches that can be found in the literature to describe the distribution of different species, populations or groups of individuals in various contexts, in space at different times, and due to local interaction and diffusion, are reaction–diffusion models. In particular, reaction–diffusion equations are often used to model spatial effects in many fields of applied mathematics, such as ecology [21–23], biology and medicine [24], economics [25], epidemiology [26,27] and social sciences [28,29]. Though these various fields and systems may seem completely different, the mathematics describing the pattern

formation in them is surprisingly similar. The study of reaction–diffusion systems may be faced using numerical or analytical methods from the theory of partial differential equations and dynamic systems. In [30], the authors considered models representing social interactions between ordinary individuals, drug users/dealers and policemen, starting from a model proposed by Epstein in [31] and introducing two modified models. They take into account an additional cross–diffusion term and some logistic effects. In the above paper, they analyze the Turing instability from an analytical point of view and increase some patterns, choosing the values of the parameters close enough to those used in [31].

In this paper, we follow this line of research, starting from the continuous model of crime introduced in [12], which incorporates the law enforcement term. In [12], the authors developed a model based on the prey–predator interaction in order to study the dynamics between the criminal and non-criminal individuals living in a specific society. More precisely, a predator–prey model with a Holling type II functional response and logistic growth rate in the non-criminal population is introduced. The considered functional response is characterized by a decelerating intake rate, which is derived from assuming that the criminally minded individuals are prevented by their capacity from victimizing the non-criminal individuals. Moreover, as law enforcement is the appropriate measure for controlling the crime rate in a community, in [12], it is considered in the criminally minded population. The role of population density in the reduction or increase in crime has been the subject of debate for a long time [32]. Whenever social, political, economic and environmental aspects are considered and observed, it is easy to find the interaction between two different and contrasting mentalities (as, for example, in the case in question: non-criminal mentality and criminal mentality) which, among other things, contributes to the degradation of society. In a given place or country, modeling how different mentalities influence criminality can be a valid starting point for scholars in the field. The basic assumption in [12] is that the only way for new criminally minded individuals to emerge is their interactions with existing criminally minded individuals. In this line of research, we place our study. $C_P(t)$ denotes the criminally minded population density and $N_P(t)$ the non-criminally minded population density at time t. In [12], the following system is introduced:

$$\begin{cases} \dfrac{dN_P}{dt} = \mu\left(1 - \dfrac{N_P}{K}\right)N_P - a\dfrac{N_P C_P}{\sigma + N_P}, \\ \dfrac{dC_P}{dt} = -\gamma C_P + b\dfrac{N_P C_P}{\sigma + N_P} - L_C C_P. \end{cases} \tag{1}$$

The parameters $\mu, a, b, \gamma, \sigma, K$ and L_C, all positive, are defined as follows:

- μ: per capita growth rate (the intrinsic rate of increase) of non-criminal individuals in the absence of criminal ones C_P;
- a: the rate at which C_P victimizes N_P (i.e., maximum capture/predation rate);
- γ: natural mortality rate of C_P in the absence of non-criminal individuals N_P;
- b: conversion rate of non-criminal population N_P into criminal population C_P;
- σ: the half saturation constant (the value at which the half of the rate constant (a) is attained);
- K: the carrying capacity of the non-criminal population in the absence of a criminal one;
- L_C: measure of the effect of the enforcement law on C_P .

Moreover, the function $\Phi = \dfrac{aN_P}{\sigma + N_P}$ denotes the rate at which the criminal population victimizes/captures the non-criminal one (the Holling type II functional response of C_P).

In particular, in [12], the authors study the existence of equilibrium points and perform analysis of linear stability. In addition, they investigate the direction and stability of Hopf bifurcation. In this paper, we generalize (1) by introducing self- and cross-diffusion terms. Self-diffusion terms model the random movements of individuals, which are conditioned by the presence/scarcity of individuals belonging to the other population in an assigned

domain. In order to include this aspect, spatial population models can contain cross-diffusion terms. The experimental analysis has highlighted that cross-diffusion can play an important role in pattern formation, also in models where self-diffusion alone does not induce spatial instability. It must certainly be said, for the sake of completeness, that, in the literature, there are various interesting models with various effects that allow for certain dynamics to be better described, such as the effects of memory, as, for example, in [33,34], by considering fractional-order models. Our aim, however, in this paper, is, starting from a continuous predator–prey model already applied in the literature, to introduce the diffusion terms and investigate the pattern formation using a simple linear stability analysis. In some cases, the explicit introduction of a space variable can modify the forecasts of the non-spatial counterpart model. The spatial diffusion plays a relevant role in the process of population evolution and in many other fields of applied mathematics ([35–45]); spatial patterns are of high relevance and importance as they may help to better describe the spatial and temporal distribution of the involved populations, thus providing important hints on the behavior of communities. Motivated by such considerations, we take into account the following system:

$$\begin{cases} \dfrac{\partial N_P}{\partial t} = \mu\left(1 - \dfrac{N_P}{K}\right)N_P - a\dfrac{N_P C_P}{\sigma + N_P} + \gamma_{11}\Delta N_P + \gamma_{12}\Delta C_P \\ \dfrac{\partial C_P}{\partial t} = -\gamma C_P + b\dfrac{N_P C_P}{\sigma + N_P} - L_C C_P + \gamma_{21}\Delta N_P + \gamma_{22}\Delta C_P \end{cases} \quad (\mathbf{x}, t) \in \Omega \times \mathbb{R}^+ \tag{2}$$

where $N_P(\mathbf{x}, t), C_P(\mathbf{x}, t)$ denote the non-criminally minded and the criminally minded population densities, respectively; $(\mathbf{x}, t)$ are the space and time variables; Ω is a bounded open subset of $\mathbb{R}^n (n = 1, 2, 3)$ with the internal cone property; Δ is the Laplacian operator; $\gamma_{ij}, i, j = 1, 2$ are the (constant) diffusion coefficients with the coercivity condition

$$\Gamma := \gamma_{11}\gamma_{22} - \gamma_{12}\gamma_{21} > 0. \tag{3}$$

The self-diffusion coefficients γ_{11} and γ_{22} are assumed as positive, while the cross-diffusion coefficients γ_{12} and γ_{21} may be positive, negative or zero.

To (2), we append the initial conditions

$$N_P(\mathbf{x}, 0) = N_P^0(\mathbf{x}), \;\; C_P(\mathbf{x}, 0) = C_P^0(\mathbf{x}), \;\; \mathbf{x} \in \Omega, \tag{4}$$

and the following homogeneous Neumann boundary conditions:

$$\nabla N_P \cdot \mathbf{n} = \nabla C_P \cdot \mathbf{n} = 0 \qquad \text{on} \qquad \partial\Omega \times \mathbb{R}^+ \tag{5}$$

with $\mathbf{n}$ being the outward unit normal vector to $\partial\Omega$.

In this paper, we focus our attention on the qualitative aspects of the mathematical modeling of crime rather than quantitative ones with data.

The plan of the paper is the following: In Section 2, the existence of socially meaningful constant steady states is analyzed, and the linear stability/instability is applied. In Section 3, the action of self- and cross-diffusion on the stability of equilibria, highlighting both the stabilizing and destabilizing effect, is investigated. The conditions guaranteeing the occurrence of Turing instability are determined, and the Turing–Hopf instabilities are investigated. Some numerical simulations, depicting the obtained results, are shown in Section 4, highlighting the rich dynamics of population interactions. In the Conclusions section (Section 5), a summary of the obtained results is presented. The paper ends with an Appendix A in which sketches of the proof of the main theorems are given.

2. Preliminaries

The constant steady solutions of (2) are the non-negative solutions of the following system:

$$\begin{cases} N_P\left[\mu\left(1-\dfrac{N_P}{K}\right)-a\dfrac{C_P}{\sigma+N_P}\right]=0 \\ C_P\left[-\gamma+b\dfrac{N_P}{\sigma+N_P}-L_C\right]=0 \end{cases} \tag{6}$$

System (6) admits the trivial equilibrium $E_0 = (0,0)$, the crime-free equilibrium $E_1 = (K,0)$ and the internal equilibrium $E^* = (N_P^*, C_P^*)$ given by

$$N_P^* = \frac{\sigma(\gamma+L_C)}{b-(\gamma+L_C)}, \quad C_P^* = \frac{\mu\sigma}{a}\left[1-\frac{\sigma(\gamma+L_C)}{K[b-(\gamma+L_C)]}\right]\left[\frac{b}{b-(\gamma+L_C)}\right]. \tag{7}$$

The condition

$$(\gamma+L_C) < \frac{Kb}{K+\sigma} \tag{8}$$

ensures that the internal equilibrium E^* is feasible.

By introducing the perturbation (N,C) to the generic spatially homogeneous equilibrium $\bar{E} = (\bar{N}_P, \bar{C}_P)$ as

$$N = N_P - \bar{N}_P, \quad C = C_P - \bar{C}_P, \tag{9}$$

from (2), the following perturbation equations can be obtained:

$$\begin{cases} \dfrac{\partial N}{\partial t} = \mu\left(1-\dfrac{2\bar{N}_P}{K}\right)N - a\left(\dfrac{\bar{N}_P}{\sigma+\bar{N}_P}\right)C + \gamma_{11}\Delta N + \gamma_{12}\Delta C + g_1, \\ \dfrac{\partial C}{\partial t} = \dfrac{\sigma b\bar{C}_P}{(\sigma+\bar{N}_P)^2}N + \left[b\left(\dfrac{\bar{N}_P}{\sigma+\bar{N}_P}\right)-(\gamma+L_C)\right]C + \gamma_{21}\Delta N + \gamma_{22}\Delta C + g_2 \end{cases} \tag{10}$$

with

$$g_1 = -\frac{\mu N^2}{K} - a(C+\bar{C}_P)f_1, \qquad g_2 = bf_1\left[C-\frac{\bar{C}_P N}{(\sigma+\bar{N}_P)}\right] \tag{11}$$

and

$$f_1 = \frac{\sigma N}{(\sigma+N+\bar{N}_P)(\sigma+\bar{N}_P)}. \tag{12}$$

Disregarding the nonlinear terms in (10), we obtain the linearized system in the neighborhood of $\bar{E} = (\bar{N}_P, \bar{C}_P)$ as follows:

$$\frac{\partial}{\partial t}\begin{pmatrix} N \\ C \end{pmatrix} = \begin{pmatrix} a_{11} & a_{12} \\ a_{21} & a_{22} \end{pmatrix}\begin{pmatrix} N \\ C \end{pmatrix} + \begin{pmatrix} \gamma_{11} & \gamma_{12} \\ \gamma_{21} & \gamma_{22} \end{pmatrix}\Delta\begin{pmatrix} N \\ C \end{pmatrix} \tag{13}$$

where

$$\begin{cases} a_{11} = \mu\left(1-\dfrac{2\bar{N}_P}{K}\right), & a_{12} = -a\left(\dfrac{\bar{N}_P}{\sigma+\bar{N}_P}\right) \\ a_{21} = \dfrac{\sigma b\bar{C}_P}{(\sigma+\bar{N}_P)^2}, & a_{22} = \left[b\left(\dfrac{\bar{N}_P}{\sigma+\bar{N}_P}\right)-(\gamma+L_C)\right], \end{cases} \tag{14}$$

and

$$\begin{pmatrix} N \\ C \end{pmatrix} = \begin{pmatrix} {N_P}^k \\ {C_P}^k \end{pmatrix}\exp(\lambda t + i\mathbf{k}\cdot\mathbf{x}) \tag{15}$$

with $\mathbf{k} = (k_x, k_y)$, $k = |\mathbf{k}| = \sqrt{k_x^2 + k_y^2}$ wavenumber. To (13), we append the following conditions:

$$\begin{cases} N(\mathbf{x}, 0) = N_0(\mathbf{x}), \ C(\mathbf{x}, 0) = C_0(\mathbf{x}), \ \mathbf{x} \in \Omega \\ \nabla C \cdot \mathbf{n} = \nabla N \cdot \mathbf{n} = 0, \ on \ \partial\Omega \times \mathbb{R}^+ . \end{cases} \tag{16}$$

When the diffusion is absent, denoted by

$$I_1^0 = a_{11} + a_{22}, \quad I_2^0 = a_{11}a_{22} - a_{12}a_{21}, \tag{17}$$

the necessary and sufficient conditions ensuring the linear stability of the generic equilibrium $\bar{E}$ are as follows [46]:

$$I_1^0 < 0, \quad I_2^0 > 0 . \tag{18}$$

Remark 1. *Let us remark that the constant steady states of (2) are the steady states of (1).*

The stability analysis and the conditions ensuring the stability of all the equilibria of (1) can be found in [12]. For the sake of completeness, such stability conditions can be summarized in the following proposition.

Proposition 1. *For system (1), the following apply:*

(i) E_0 *is always unstable;*

(ii) E_1 *is stable if* $L_C > -\gamma + \dfrac{Kb}{K+\sigma}$;

(iii) If we assume (8) holds, then E^* *exists, and it is stable if* $L_C > -\gamma + \dfrac{Kb}{K+2\sigma}$, *while it is unstable if* $L_C < -\gamma + \dfrac{Kb}{K+2\sigma}$.
Moreover, the Hopf bifurcation occurs at point E^* *in system (1) when*

$$L_C = -\gamma + \frac{Kb}{K+2\sigma}. \tag{19}$$

Remark 2. *It is worth highlighting that the stability condition for* E_1 *implies the non-existence of the internal equilibrium* E^*.

Remark 3. *Using (14), evaluated for* E^*, *it follows that* $a_{22} = 0$. *Then,* $I_2^0(E^*) = -a_{12}a_{21} > 0$ *for all values of parameters, ensuring the existence of the internal equilibrium. The necessary and sufficient condition for linear stability of* E^* *reduces to* $I_1^0(E^*) = a_{11} < 0$ *according to Proposition 1.*

Remark 4. *In view of (iii) of Proposition 1 and Remark 3, the spatially homogeneous equilibrium* E^*, *(linearly) stable for* $I_1^0(E^*) < 0$, *loses its stability when* $I_1^0(E^*) = 0$, *and a limit cycle can arise surrounding the unstable steady state for* $0 < I_1^0(E^*) << 1$. *The periodic solution has period* $T = \frac{2\pi}{\omega}$, *where* $\omega = \sqrt{I_2^0(E^*)}$ *is the angular frequency.*

3. Diffusion-Driven Stability/Instability

Now, we consider system (2) with diffusion. In particular, we refer to the perturbation systems (13)–(16) linearized around $\bar{E}$.

The characteristic equation which provides the eigenvalue λ as a function of the wavenumber k is

$$\lambda^2 - I_1\lambda + I_2 = 0 \tag{20}$$

with

$$\begin{cases} I_1 = I_1^0 - k^2(\gamma_{11} + \gamma_{22}) \\ I_2 = \Gamma k^4 + q_{\bar{E}} k^2 + I_2^0 \end{cases} \tag{21}$$

and

$$q_{\bar{E}} = \gamma_{21}a_{12} + \gamma_{12}a_{21} - \gamma_{22}a_{11} - \gamma_{11}a_{22}. \tag{22}$$

The effect of self- and cross-diffusion on the stability of E_0, E_1 is summarized in the following theorems.

For the sake of completeness, a sketch of the proofs of all the following theorems is given in Appendix A.

Theorem 1. *E_0, unstable in the absence of diffusion, is stabilized by the action of self- and cross-diffusion if and only if*

$$\begin{cases} k^2(\gamma_{11} + \gamma_{22}) + (\gamma + L_C) > \mu \\ \Gamma k^4 + [(\gamma + L_C)\gamma_{11} - \mu\gamma_{22}]k^2 - \mu(\gamma + L_C) > 0 \end{cases} \tag{23}$$

Theorem 2. *E_1, stable in the absence of diffusion when $L_C > -\gamma + \dfrac{Kb}{K+\sigma}$, is destabilized by the action of self- and cross-diffusion if and only if*

$$\Gamma k^4 + \left[\mu\gamma_{22} - \gamma_{11}(-\gamma - L_C + \frac{bK}{K+\sigma}) - \gamma_{21}\frac{aK}{K+\sigma}\right]k^2 - \mu(-\gamma - L_C + \frac{bK}{\sigma+K}) < 0. \tag{24}$$

Remark 5. *Let us remark that a necessary condition ensuring that (24) is satisfied is $\gamma_{21} > 0$. In addition, from (24), it is evident that self-diffusion alone does not induce instability.*

Let us observe that, if L_C is sufficiently large, according to (ii) of Proposition 1, E_1 is stable. Therefore, $L_C^{thr} = -\gamma + \dfrac{Kb}{K+\sigma}$ can be seen as a threshold value above which the crime-free equilibrium is stable. Figure 1 highlights the behavior of N_P (solid lines) and C_P (dashed lines) as a function of time for different values of the measure of the enforcement law L_C. Here, model parameters are as in Table 1, and $E_1 \equiv (6, 0)$, and $L_C^{thr} = 0.58$.

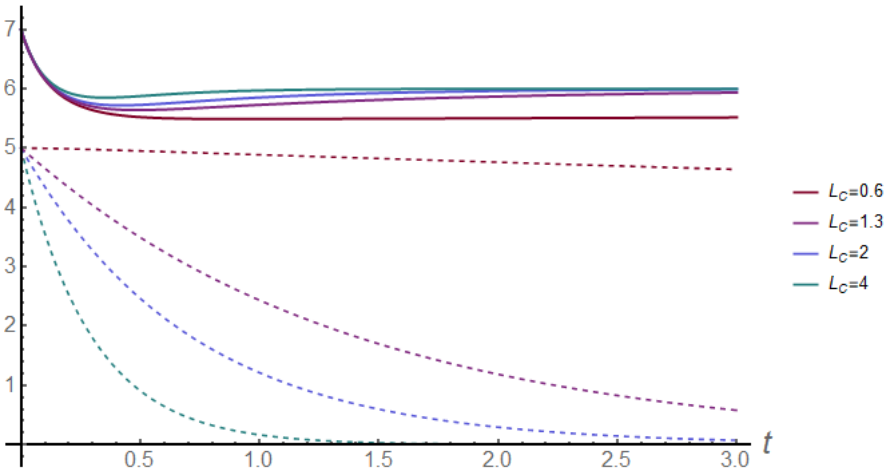

Figure 1. Plots of N_P (solid lines) and $C_P(t)$ (dashed lines) as function of time for different values of the measure of the enforcement law $L_C > L_C^{thr} = 0.58$. Here, $N_P(0) = 7$, and $C_P(0) = 5$. Model parameters are as in Table 1, and $E_1 \equiv (6, 0)$.

Table 1. Fixed values for some model parameters in numerical simulations.

Parameters	μ	K	σ	a	γ	b	L_C
Values	8	6	1	0.9	0.23	0.95	0.46

From this point on, we consider the internal equilibrium E^*. Evaluated for E^*, (22) becomes

$$q_{E^*} = -\mu\frac{Kb-(\gamma+L_C)(K+2\sigma)}{K[b-(\gamma+L_C)]}\gamma_{22}+\frac{\mu\gamma_{12}}{K}[Kb-(\gamma+L_C)(K+\sigma)]-\frac{a\gamma_{21}}{b}(\gamma+L_C). \quad (25)$$

The following theorem holds.

Theorem 3. *Let us assume that (8) holds. Then, E^*, unstable in the absence of diffusion for $L_C < -\gamma+\frac{Kb}{K+2\sigma}$, is stabilized by the action of self- and cross-diffusion if and only if*

$$\begin{cases} k^2(\gamma_{11}+\gamma_{22}) > \mu\dfrac{Kb-(\gamma+L_C)(K+2\sigma)}{K[b-(\gamma+L_C)]} \\ \\ \Gamma k^4+q_{E^*}k^2+I_2^0(E^*)>0 \end{cases} \quad (26)$$

where q_{E^*} is given by (25).

Remark 6. *Since $I_2^0(E^*) > 0$, then $q_{E^*} > 0$ is a sufficient condition ensuring that $(26)_2$ is satisfied.*

In view of Remark 6, denoted by

$$A_1 = \frac{\mu}{K}[Kb-(\gamma+L_C)(K+\sigma)]\frac{\gamma_{12}}{\gamma_{22}}-\frac{a}{b}(\gamma+L_C)\frac{\gamma_{21}}{\gamma_{22}}, \qquad B_1 = k^2\frac{(\gamma_{11}+\gamma_{22})}{\gamma_{22}}, \quad (27)$$

the following theorem holds.

Theorem 4. *Let us assume that (8) holds. Then, if $L_C < -\gamma+\frac{Kb}{K+2\sigma}$, a sufficient condition guaranteeing that E^*, unstable in the absence of diffusion, is stabilized by the action of self- and cross-diffusion is given by*

$$\mu\frac{Kb-(\gamma+L_C)(K+2\sigma)}{K[b-(\gamma+L_C)]} < \min\{A_1, B_1\}, \quad (28)$$

with A_1, B_1 defined as in (27).

Now we are looking for conditions ensuring that the coexistence equilibrium E^*, stable when the diffusion is absent, becomes unstable when the effect of diffusion is considered.

We observe that the self-diffusion alone ($\gamma_{12} = \gamma_{21} = 0$) does not lead to the occurrence of Turing instability.

Since $I_1^0(E^*) < 0$ implies $I_1(E^*) < 0$ for all k, Turing instability may occur only if $I_2(E^*) < 0$ for mode $k \neq 0$. A necessary condition for the occurrence of Turing instability is $q_{E^*} < 0$.

The condition for the marginal stability at $k^2 = k_{cr}^2$ is $\min(I_2(k_{cr}^2)) = 0$. Such a minimum value of $I_2(k^2)$ is reached at $k_{cr}^2 = -\frac{q_{E^*}}{2\Gamma}$.

In addition, $I_2(k_{cr}^2) < 0$ gives $q_{E^*}^2 - 4\Gamma I_2^0(E^*) > 0$. Then, the conditions for the occurrence of cross-diffusion-driven instability for E^* can be summarized in the following main theorem.

Theorem 5. *Let us assume that (8) and (3) hold. The conditions for cross-diffusion-driven instability of the homogeneous steady state E^* are given by*

$$\begin{cases} a_{11} < 0, \qquad a_{12}\gamma_{21}+a_{21}\gamma_{12}-a_{11}\gamma_{22} < 0, \\ \\ (a_{12}\gamma_{21}+a_{21}\gamma_{12}-a_{11}\gamma_{22})^2 > -4(\gamma_{11}\gamma_{22}-\gamma_{12}\gamma_{21})a_{12}a_{21}. \end{cases} \quad (29)$$

The above inequalities (29) define a region where the coexistence equilibrium E^* is unstable. When choosing γ_{12} as bifurcation parameter and $\gamma_{12} = \gamma_{12}^{cr}$ as the Turing threshold, bifurcation happens at the critical value

$$\gamma_{12}^{cr} = \frac{a_{12}\gamma_{21} + a_{11}\gamma_{22} + 2\sqrt{a_{12}\gamma_{22}(a_{11}\gamma_{21} - a_{21}\gamma_{11})}}{a_{21}} \tag{30}$$

corresponding with the critical wavenumber

$$k_{cr}^2 = \sqrt{-\frac{a_{12}a_{21}}{\gamma_{11}\gamma_{22} - \gamma_{12}\gamma_{21}}} \neq 0. \tag{31}$$

For $\gamma_{12} > \gamma_{12}^{cr}$, the unstable wavenumbers stay in between the roots k_-^2, k_+^2, the roots of $I_2(k^2) = 0$. We conclude this section by highlighting the existence of the Turing–Hopf bifurcation at the point of intersection of the Hopf and Turing bifurcation curves. In the vicinity of this point, it is possible to observe both the formation of inhomogeneous stationary patterns generated by Turing instabilities and the occurrence of homogeneous oscillations generated by the Hopf bifurcation. This coexistence can lead to the eventual appearance of an interesting class of spatio-temporal behaviors. When the kinetics of system (1) exhibits a Hopf bifurcation ($0 < I_1^0(E^*) << 1$), highlighting a limit cycle, if $I_1(E^*) < 0$, $I_2(E^*) < 0$, then weak Turing–Hopf instabilities appear. These instabilities are represented as slight oscillations which have the frequency of the cycle solution superimposed on a predominantly inhomogeneous pattern. It is observed that these oscillations increase with increasing amplitude of the limit cycle, that is, with increasing $I_1^0(E^*)$.

4. Numerical Simulations

In this paper, an analytical study of the interaction of two spatially distributed populations, the criminally minded population and the non-criminally minded one, has been performed. In order to show the theoretical results and highlight the effect of diffusion on the behavior of populations, in this section, we provide some numerical simulations. First, we fix values to γ_{11}, γ_{22} and γ_{21}. We choose γ_{12} as a bifurcation parameter. According to Theorem 5, from (30), we obtain γ_{12}^{cr} as the minimum value for Turing instability to occur. Figure 2 depicts the plots of $I_2(k^2)$ for different values of the bifurcating parameter γ_{12}. Specifically, we have chosen $\gamma_{11} = 0.8, \gamma_{22} = 2, \gamma_{21} = 3$ and other parameter values as shown in Table 1. In this case, $\gamma_{12}^{cr} \approx -4.445$. As we can see, for $\gamma_{12} = -4.0 > \gamma_{12}^{cr}$, the graph shows that the curve does not intersect the horizontal axis, and, consequently, there are no unstable modes. As γ_{12} decreases, the interval of unstable modes increases as well. Analogously, as the bifurcation parameter decreases, the real part of the corresponding eigenvalue $\lambda(k)$ becomes positive (right panel of Figure 2).

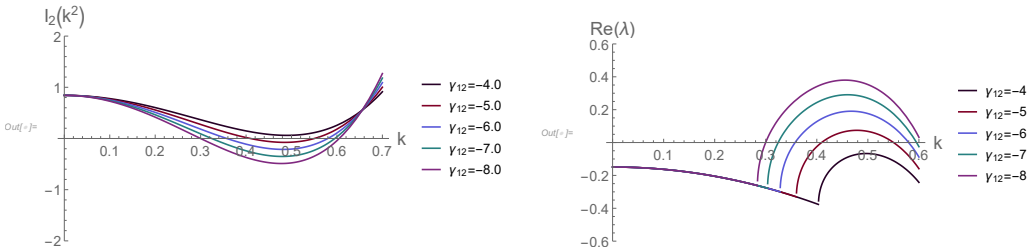

Figure 2. Left panel: plots of $I_2(k^2)$ as function of the wavenumber for various values of the bifurcation parameter γ_{12}; right panel: plots of the real part of the eigenvalue $\lambda(k)$, defined in (20) as function of the wavenumber for various values of γ_{12}. Here, $\gamma_{11} = 0.8, \gamma_{22} = 2, \gamma_{21} = 3$ and other parameters as shown in Table 1.

We have solved system (2) in the domain $\Omega = [0, 40] \times [0, 40]$ with initial conditions (4) and homogeneous Neumann boundary conditions (5). The initial data have been chosen as a random perturbation of the coexistence equilibrium. For the spatial discretization, we use

finite differences with step $h = 0.2$. For the time discretization, we use the explicit Euler's method, with the time step varying from 10^{-4} to 10^{-5} depending on the parameters. We have considered the model parameters shown in Table 1. Figures 3–6 show snapshots of patterns which depict different possible scenarios. In every pattern, the blue color represents the low density of the population, and the yellow color represents the high density of that population. By various numerical simulations, we have observed that both populations are distributed predominantly over the entire domain, with some very low-density patches, generating predominantly spot patterns. Socially, yellow spots on a blue background (see Figure 6) represent that the criminally minded population exists in isolated regions with high density, motivated, for example, by the need to cooperate with other criminal individuals. For Figures 3 and 4, we have chosen negative cross-diffusion coefficients ($\gamma_{12} = -0.8, \gamma_{21} = -0.1$ and $\gamma_{12} = -3, \gamma_{21} = -1$, respectively) and other diffusion coefficients ($\gamma_{11} = 0.3, \gamma_{22} = 0.5$ and $\gamma_{11} = 2, \gamma_{22} = 2$, respectively). In such figures, as the spread of individuals from both populations increases, it is observed that the disposition of the spots becomes more regular. For Figure 5, we have chosen a negative cross-diffusion coefficient $\gamma_{12} = -5$ and other diffusion coefficients as follows: $\gamma_{11} = 0.8, \gamma_{22} = 2, \gamma_{21} = 3$, satisfying the conditions of the Turing instability region. For Figure 6, we have chosen positive cross-diffusion coefficients $\gamma_{12} = 1, \gamma_{21} = 3.9$ and other diffusion coefficients as follows: $\gamma_{11} = 2, \gamma_{22} = 2$, satisfying the conditions of the Turing instability region. This choice of positive γ_{12} (γ_{21}) depicts the social scenario in which the non-criminally minded population (criminally minded population) gravitates towards regions with a lower concentration of criminally minded individuals (non-criminally minded population).

It is interesting to note that, in this last case (Figure 6), it is possible to observe a duality, wherein non-criminally minded individuals live in regions without criminally minded individuals and vice versa. Instead, in the other cases (Figures 3–5), the patterns share the property wherein both criminally minded and non-criminally minded individuals coexist in the same region.

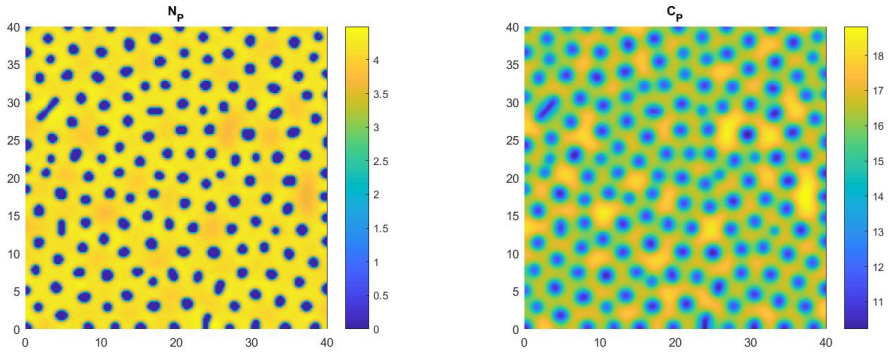

Figure 3. Snapshots of patterns of the non-criminally minded population and criminally minded population with $\gamma_{11} = 0.3, \gamma_{22} = 0.5, \gamma_{21} = -0.1, \gamma_{12} = -0.8$ and other parameters as in Table 1.

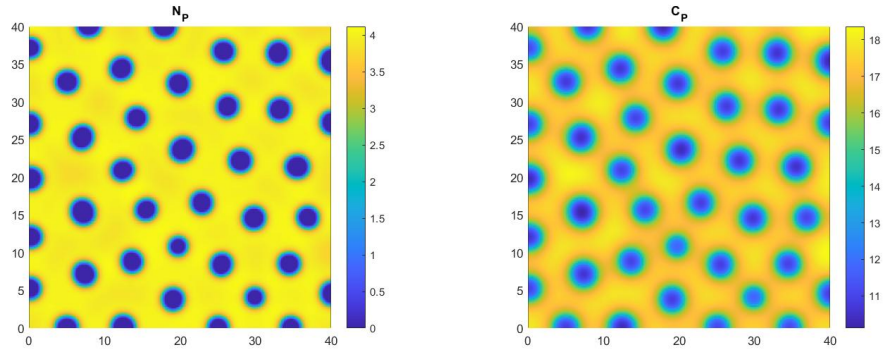

Figure 4. Snapshots of patterns of the non-criminally minded population and criminally minded population with $\gamma_{11} = 2, \gamma_{22} = 2, \gamma_{21} = -1, \gamma_{12} = -3$ and other parameters as shown in Table 1.

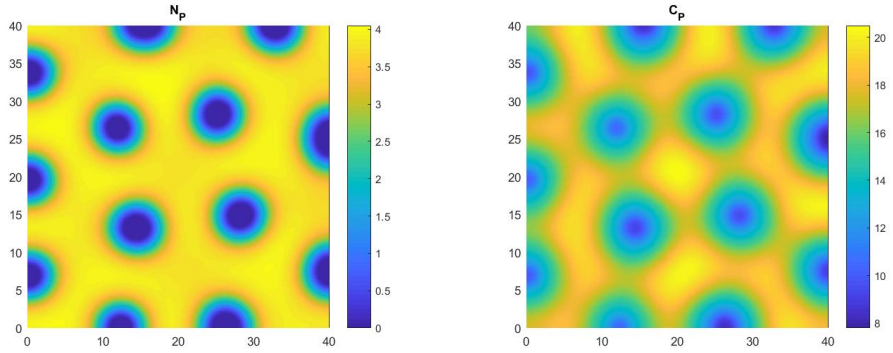

Figure 5. Snapshots of patterns of the non-criminally minded population and criminally minded population with $\gamma_{11} = 0.8, \gamma_{22} = 2, \gamma_{21} = 3, \gamma_{12} = -5$ and other parameters as shown in Table 1.

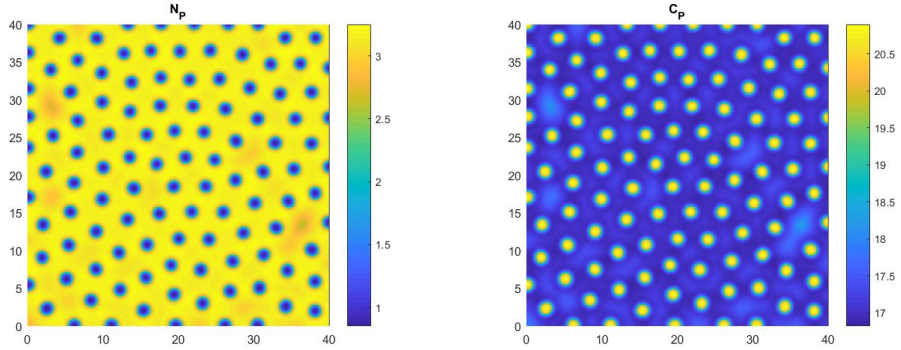

Figure 6. Snapshots of patterns of the non-criminally minded population and criminally minded population with $\gamma_{11} = 2, \gamma_{22} = 2, \gamma_{21} = 3.9, \gamma_{12} = 1$ and other parameters as shown in Table 1.

We end this section by considering the region around the Turing–Hopf bifurcation. We perform simulations for a parameter set of interest. When we choose $L_C = 0.4$ and set other parameters as shown in Table 1, (19) is satisfied, and the coexistence equilibrium $E^* = (1.97, 17.73)$ is oscillatory, exhibiting limit cycles. In Figure 7 (right panel), a plot of the limit cycle in the phase plane (with initial conditions $(N_P(0), C_P(0)) = (0.5, 5)$) is shown. The left panel of the same figure shows the time evolution of both criminally minded and non-criminally minded populations.

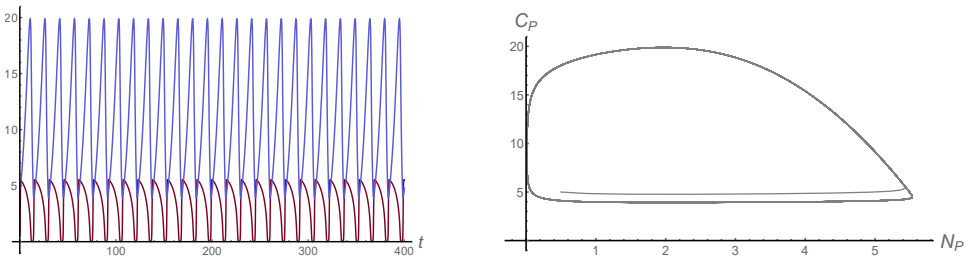

Figure 7. In the left panel, trajectories of system (1) with $L_C = 0.4$ guarantee that (19) holds, and other parameters are set as shown in Table 1. Blue and red lines represent $N_P(t)$ and $C_P(t)$, respectively, as a function of time t. Here, the system shows persistent oscillations. In the right panel, the corresponding phase plane plot clearly shows the limit cycle.

Keeping the same parameter values as in Figure 7, we simulate the corresponding diffusive model (2). For the sake of completeness, it should be clarified that both 1D and 2D experiments have been performed, but we prefer to show only the results for the 1D setting with the intention of highlighting the complete trajectories of both populations since the graphs for the 2D setting could only be obtained at certain fixed instants of time. Various numerical experiments with different sets of diffusion coefficients (satisfying the Turing conditions) allowed us to observe that the same type of instability observed

in the ODE model persists, and the system still shows an oscillatory behavior. Figure 8 reports the trajectories for the non-criminally minded and criminally minded populations up to $T = 800$, with $\gamma_{11} = 0.5, \gamma_{22} = 2, \gamma_{12} = 0.4, \gamma_{21} = -1.5$. As evidenced by the numerical simulations conducted, spatial diffusion can deeply influence the behavior of social dynamics.

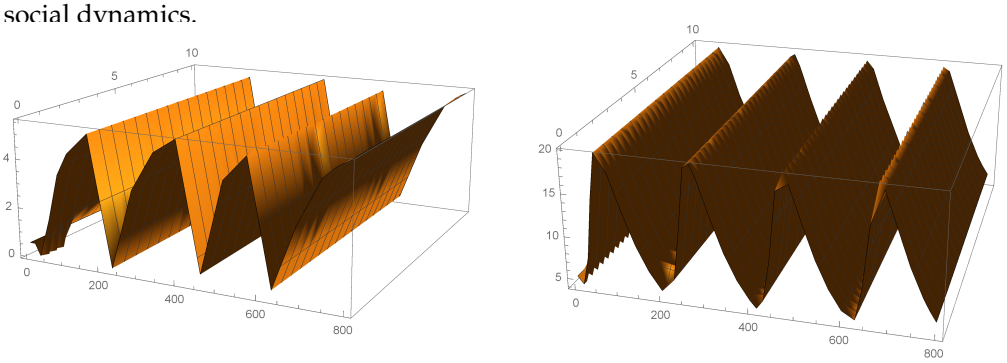

Figure 8. Numerical simulation of system (2) in presence of diffusion ($\gamma_{11} = 0.5, \gamma_{22} = 2, \gamma_{12} = 0.4$, $\gamma_{21} = -1.5$), satisfying the Turing–Hopf conditions. Here, $L_C = 0.4$, and other parameters are set as shown in Table 1. Complete trajectory of non-criminally minded population (left panel) and criminally minded population (right panel) up to $T = 800$.

5. Conclusions

In this paper, a generalized crime model is introduced to describe the interaction between non-criminally minded and criminally minded populations. In particular, random movement of both populations is allowed. The more general case in which the diffusion of one population depends on the movement of the other population is analyzed (cross-diffusion system). This study shows the importance of considering population movement and spatial heterogeneity (which is nowadays well known and recognized in many fields) in the analysis of social interactions. In some cases, the explicit introduction of spatial diffusion can modify the forecasts of the non-spatial counterpart model. A linear instability analysis of the coexistence equilibrium (when it exists) is performed. In particular, conditions guaranteeing cross-diffusion-induced instability have been determined. Numerical simulations performed on the obtained results are shown. In particular, by varying the values of the diffusion coefficients, Turing patterns emerge, representing a spatial redistribution of the population in the environment. Destabilizing mechanisms of the coexistence equilibrium and some investigations for the possible oscillatory phenomena are applied. Extensive numerical simulations highlighting such interesting dynamics are performed.

Author Contributions: Conceptualization, I.T. and M.V.; formal analysis, I.T. and M.V.; Investigation, I.T. and M.V.; writing—original draft, I.T. and M.V.; writing—review & editing, I.T. and M.V. All authors have read and agreed to the published version of the manuscript.

Funding: This research received no external funding.

Data Availability Statement: No new data were created or analyzed in this study. Data sharing is not applicable to this article.

Acknowledgments: This paper has been performed under the auspices of the Gruppo Nazionale per la Fisica Matematica (GNFM) of Istituto Nazionale di Alta Matematica (INdAM). Authors thank the Editor and anonymous referees for their accuracy and constructive comments.

Conflicts of Interest: The authors declare no conflicts of interest.

Appendix A

Proof of Theorem 1. Evaluating (14) in E_0, it follows that

$$\begin{cases} a_{12}(E_0) = a_{21}(E_0) = 0, \\ a_{11}(E_0) = \mu, \quad a_{22}(E_0) = -(\gamma + L_C). \end{cases} \tag{A1}$$

By using the Routh–Hurwitz conditions, the thesis is immediately obtained from (21)–(22). □

Proof of Theorem 2. Since $I_1^0(E_1) < 0$ implies $I_1(E_1) < 0$, instability in presence of self- and cross-diffusion occurs only if $I_2(E_1) < 0$. Evaluating (14) in E_1, one obtains

$$\begin{cases} a_{11}(E_1) = -\mu, \quad a_{12}(E_1) = -a\dfrac{K}{\sigma + K}, \\ a_{12}(E_1) = 0, \qquad a_{22}(E_1) = \dfrac{bK}{\sigma + K} - (\gamma + L_C), \end{cases} \tag{A2}$$

and the Condition (24) immediately follows. □

Proof of Theorem 3. Evaluating (14) in E^*, one obtains

$$\begin{cases} a_{11}(E^*) = \mu\left(1 - \dfrac{2\sigma(\gamma + L_C)}{K(b - (\gamma + L_C))}\right), \quad a_{12}(E^*) = -\dfrac{a}{b}(\gamma + L_C), \\ a_{21}(E^*) = \dfrac{\mu}{K}[Kb - (\gamma + L_C)(k + \sigma)], \quad a_{22}(E^*) = 0, \end{cases} \tag{A3}$$

and, by using Routh–Hurwitz conditions, the proof immediately follows. □

Proof of Theorem 4. The thesis immediately follows from Theorem 3 and Remark 6. □

References

1. Snijders, T.; Baerveldt, C. A multilevel network study of the effects of delinquent behavior on friendship evolution. *J. Math. Sociol.* **2003**, *27*, 123–151. [CrossRef]
2. Appiahene, G. Violent crime in Ghana: The case of robbery. *Ghana J. Crim. Justice* **1998**, *26*, 409–424. [CrossRef]
3. Entorf, H.; Spengler, H. Socioeconomic and demographic factors of crime in Germany: Evidence from panel data of the german states. *Int. Rev. Law Econ.* **2000**, *20*, 75–106. [CrossRef]
4. Becker, G. Crime and punishment: An economic approach. *J. Political Econ.* **1968**, *76*, 169–217. [CrossRef]
5. Harries, K. The geography of American crime. *J. Geogr.* **1971**, *70*, 204–213.
6. Ibrahim, O.; Okuonghae, D.; Ikhile, M. Mathematical Modeling of the Population Dynamics of Age-Structured Criminal Gangs with Correctional Intervention Measures. *Appl. Math. Model.* **2022**, *107*, 39–71. [CrossRef]
7. Nuno, J.; Herrero, M.; Primicerio, M. A triangle model of criminality. *Phys. A* **2008**, *12*, 2926–2936. [CrossRef]
8. Abbas, S.; Tripathi, J.; Anam, N. Dynamical analysis of a model of social behaviour: Criminal versus non-criminal population. *Chaos Solitons Fractals* **2017**, *15*, 121–129. [CrossRef]
9. González-Parra, G.; Chen-Charpentier, B.; Kojouharov, H.V. Mathematical modeling of crime as a social epidemic. *J. Interdiscip. Math.* **2018**, *21*, 623–643. [CrossRef]
10. Lacey, A.A.; Tsardakas, M.N. A mathematical model of serious and minor criminal activity. *Eur. J. Appl. Math.* **2016**, *27*, 403–421. [CrossRef]
11. Kwofie, T.; Dogbatsey, M.; Moore, S. Curtailing crime dynamics: A mathematical approach. *Front. Appl. Math. Stat.* **2023**, *8*, 1086745. [CrossRef]
12. Tripathi, J.; Bugalia, S.; Burdak, K.; Abbas, S. Dynamical analysis and effects of law enforcement in a social interaction model. *Phys. A* **2021**, *567*, 125725. [CrossRef]
13. Cantrell, R.S.; Cosner, C.; Manasevich, R. Global bifurcation of solutions for crime modelling equations. *SIAM J. Math. Anal.* **2012**, *44*, 1340–1358. [CrossRef]
14. Jones, P.A.; Brantincham, P.; Chayes, L.R. Statistical model of criminal behaviour: The effect of law enforcement actions. *Math. Model. Method Appl. Sci.* **2010**, *20*, 1397–1423. [CrossRef]

15. Short, M.B.; Brantingham, P.J.; Bertozzi, L.; Tita, G.E. Dissipation and displacement of hotspots in reaction-diffusion models of crime. *Proc. Nat. Accad. Sci. USA* **2010**, *107*, 3961–3965. [CrossRef] [PubMed]
16. Short, M.B.; Bertozzi, L.; Brantingham, P.J. Nonlinear patterns in urban crime: Hotspots, bifurcations and suppression. *SIAM J. Appl. Dyn. Syst.* **2010**, *9*, 462–483. [CrossRef]
17. Brantingham, P.; Brantingham, P. *Patterns in Crime*; Macmillan: New York, NY, USA, 1984.
18. Berestycki, H.; Rodríguez, N.; Ryzhik, L. Traveling Wave Solutions in a Reaction-Diffusion Model for Criminal Activity. *Multiscale Model. Simul.* **2013**, *11*, 1097–1126. [CrossRef]
19. Basilio, M.P.; Pereira, V.; Ygit, F. New Hybrid EC-Promethee Method with Multiple Iterations of Random Weight Ranges: Applied to the Choice of Policing Strategies. *Mathematics* **2023**, *11*, 4432. [CrossRef]
20. Short, M.B.; D'Orsogna, M.R.; Pasour, V.; Chayes, B. A Statistical Model of Criminal Behavior. *Math. Model. Methods Appl. Sci.* **2008**, *18*, 249–1267. [CrossRef]
21. Kan-on, Y.; Mimura, M. Singular perturbation approach to a 3-component reaction-diffusion system arising in population dynamics. *SIAM J. Math. Anal.* **1998**, *29*, 1519–1536. [CrossRef]
22. Kabir, M.H.; Gani, M.O. Numerical bifurcation analysis and pattern formation in a minimal reaction-diffusion model for vegetation. *J. Theor. Biol.* **2022**, *536*, 110997. [CrossRef] [PubMed]
23. Sherratt, J. Pattern solutions of the Klausmeier model for banded vegetation in semiarid environments v: The transition from patterns to desert. *SIAM J. Appl. Math.* **2013**, *73*, 1347–1367. [CrossRef]
24. Lombardo, M.; Barresi, R.; Bilotta, E.; Gargano, F.; Pantano, P.; Sammartino, M. Demyelination patterns in a mathematical model of multiple sclerosis. *J. Math. Biol.* **2017**, *75*, 373–417. [CrossRef] [PubMed]
25. Rionero, S.; Torcicollo, I. On the dynamics of a nonlinear reaction–diffusion duopoly model. *Int. J. Non-Linear Mech.* **2018**, *99*, 105–111. [CrossRef]
26. Wang, W.; Cai, Y.; Wu, M.; Wang, K.; Li, Z. Complex dynamics of a reaction–diffusion epidemic model. *Nonlinear Anal. Real World Appl.* **2012**, *13*, 2240–2258. [CrossRef]
27. Avila-Vales, E.; Perez, A. Dynamics of a reaction-diffusion sirs model with general incidence rate in a heterogeneous environment. *Z. Angew. Math. Phys.* **2021**, *73*, 9. [CrossRef] [PubMed]
28. Petrovskii, S.; Alharbi, W.; Alhomairi, A.; Morozov, A. Modelling population dynamics of social protests in time and space: The reaction-diffusion approach. *Mathematics* **2020**, *8*, 78. [CrossRef]
29. Wen, Z.; Fu, S. Global solutions to a class of multi-species reaction-diffusion systems with cross-diffusions arising in population dynamics. *J. Comput. Appl. Math.* **2009**, *230*, 34–43. [CrossRef]
30. Inferrera, G.; Munafò, C.; Oliveri, F.; Rogolino, P. Reaction-diffusion models of crimo–taxis in a street. *Appl. Math. Comput.* **2024**, *467*, 34–43. [CrossRef]
31. Epstein, J.M. *Nonlinear Dynamics, Mathematical Biology, and Social Science*; Addison-Wesley: Reading, MA, USA, 1997.
32. Fung, W.; Keung, K. An investigation of stochastic analysis of flexible manufacturing system simulation. *Int. J. Adv. Manuf. Technol.* **1999**, *15*, 244–250.
33. Pritam, K.S.; Mathur, T.; Agarwal, S. Underlying dynamics of crime transmission with memory. *Chaos Solitons Fractals* **2021**, *146*, 110838. [CrossRef]
34. Arora, S.; Mathur, T.; Tiwari, K. A fractional-order model to study the dynamics of the spread of crime. *J. Comput. Appl. Math.* **2023**, *426*, 115102. [CrossRef]
35. Rionero, S.; Torcicollo, I. On an ill-posed problem in nonlinear heat conduction. *Transp. Theory Stat. Phys.* **2000**, *29*, 173–186. [CrossRef]
36. Torcicollo, I. Su alcuni problemi di diffusione non lineare. *Boll. Unione Mat. Ital. A* **2000**, *3*, 407–410.
37. Triska, A.; Gunawan, A.; Nuraini, N. The Effects of the Susceptible and Infected Cross-Diffusion Terms on Pattern Formations in an SI Model. *Mathematics* **2023**, *11*, 3745. [CrossRef]
38. Carfora, M.; Torcicollo, I. Cross-diffusion-driven instability in a predator-prey system with fear and group defense. *Mathematics* **2020**, *8*, 1244. [CrossRef]
39. Gambino, G.; Lombardo, M.; Lupo, S.; Sammartino, M. Super-critical and sub-critical bifurcations in a reaction-diffusion Schnakenberg model with linear cross-diffusion. *Ric. Mat.* **2016**, *65*, 449–467. [CrossRef]
40. Alì, G.; Bilotta, E.; Chiaravalloti, F.; Pantano, P.; Pezzi, O.; Scuro, C.; Valentini, F. Spatiotemporal Pattern formation in a ring of Chua's oscillators. *Regul. Chaotic Dyn.* **2021**, *26*, 717–731. [CrossRef]
41. De Angelis, M.; Fiore, G. Diffusion effects in a superconductive model. *Commun. Pure Appl. Anal.* **2014**, *13*, 217–223. [CrossRef]
42. Rionero, S.; Vitiello, M. Long-time behaviour of the solutions of Murray-Thomas model for interacting chemicals. *Math. Comput. Simul.* **2012**, *82*, 1597–1614. [CrossRef]
43. Ramella, G.; di Baja, G.S. From color quantization to image segmentation. In Proceedings of the 2016 12th International Conference on Signal-Image Technology & Internet-Based Systems (SITIS), Naples, Italy, 28 November–1 December 2016; pp. 798–804.
44. Rionero, S.; Vitiello, M. Stability and absorbing set of parabolic chemotaxis model of Esccheria coli. *Nonlinear Anal. Model. Control.* **2013**, *18*, 210–226. [CrossRef]

45. Rionero, S.; Vitiello, M. On the dynamics of the Lengyel–Epstein model with forcing intensity. *Ric. Mat.* **2018**, *67*, 739–754. [CrossRef]
46. Merkin, D. *Introduction to the Theory of Stability*; Texts in Applied Mathematics; Springer: Berlin/Heidelberg, Germany, 1997; Volume 24.